Neuron
Article

A Whole-Brain Atlas of Inputs to Serotonergic Neurons of the Dorsal and Median Raphe Nuclei

Iskra Pollak Dorocic,[1] Daniel Fürth,[1] Yang Xuan,[1] Yvonne Johansson,[1] Laura Pozzi,[1] Gilad Silberberg,[1] Marie Carlén,[1] and Konstantinos Meletis[1,*]
[1]Department of Neuroscience, Karolinska Institutet, 17177 Stockholm, Sweden
*Correspondence: dinos.meletis@ki.se
http://dx.doi.org/10.1016/j.neuron.2014.07.002

SUMMARY

The serotonin system is proposed to regulate physiology and behavior and to underlie mood disorders; nevertheless, the circuitry controlling serotonergic neurons remains uncharacterized. We therefore generated a comprehensive whole-brain atlas defining the monosynaptic inputs onto forebrain-projecting serotonergic neurons of dorsal versus median raphe based on a genetically restricted transsynaptic retrograde tracing strategy. We identified discrete inputs onto serotonergic neurons from forebrain and brainstem neurons, with specific inputs from hypothalamus, cortex, basal ganglia, and midbrain, displaying a greater than anticipated complexity and diversity in cell-type-specific connectivity. We identified and functionally confirmed monosynaptic glutamatergic inputs from prefrontal cortex and lateral habenula onto serotonergic neurons as well as a direct GABAergic input from striatal projection neurons. In summary, our findings emphasize the role of hyperdirect inputs to serotonergic neurons. Cell-type-specific classification of connectivity patterns will allow for further functional analysis of the diverse but specific inputs that control serotonergic neurons during behavior.

INTRODUCTION

The serotonin (5-hydroxytryptamine [5-HT]) system has been linked to regulation of emotional states, underlying the etiology as well as treatment of mood disorders (Lucki, 1998; Paul and Lowry, 2013). In addition, dysfunction of the serotonin system has been implicated in schizophrenia, drug addiction, Parkinson's disease, and autism (Abi-Dargham et al., 1997; Huot et al., 2011; Nakamura, 2013).

The serotonin system has been hypothesized to regulate a number of behaviors, notably involving aggression and aversive learning, impulsivity, attention, decision making, and reward (Abi-Dargham et al., 1997; Clarke et al., 2004; Cools et al., 2008; Dayan and Huys, 2009; Homberg, 2012; Nakamura, 2013). How these behaviors are directly shaped by serotonin and how distinct long-range or local inputs onto subsets of serotonergic neurons define the wide behavioral repertoire is currently unknown.

Investigation of the anatomy of the serotonin system has revealed cell-type diversity and specificity in the projection patterns (Abrams et al., 2004; Hale and Lowry, 2011; Vertes and Linley, 2008). The midbrain dorsal raphe (DR) and median raphe (MR) nuclei contain the major serotonergic populations (Dahlstroem and Fuxe, 1964) and display ascending projections targeting a large number of forebrain regions (Azmitia and Segal, 1978; Fuxe, 1965; Vertes and Linley, 2008). Despite the apparent specialization of the DR and MR serotonergic topographic projections pattern and physiology, the inputs these regions receive are considered to be similar (Vertes and Linley, 2008).

Recordings from DR neurons including that of putative serotonergic neurons show variable responses to stimuli and activity modulated by behavioral state (Jacobs and Azmitia, 1992; Ranade and Mainen, 2009; Trulson and Jacobs, 1979; Veasey et al., 1997). Overall, serotonergic neurons show heterogeneous and dynamic changes in their firing patterns, most likely representing the underlying dynamics of their diverse synaptic inputs.

Serotonergic neurons make up a minority of the neuronal population in the DR and MR (Fu et al., 2010; Jacobs and Azmitia, 1992), in addition to known populations of peptidergic, dopaminergic, and GABAergic neurons located in the local network, although the full molecular or functional heterogeneity of these neuronal populations has not been determined (Fu et al., 2010; Kirby et al., 2003; Ochi and Shimizu, 1978; Stratford and Wirtshafter, 1990). Histological quantification places the number of serotonergic neurons in DR to 25%–50% and in MR to 20%–30% of the total neuronal population (Descarries et al., 1982; Steinbusch et al., 1980). Therefore, to determine the logic underlying circuit structure and function, it is necessary to determine circuit connectivity based on inputs to a defined neuron type rather than to a defined anatomical region.

Conventional tracing approaches have been invaluable in the characterization of the major brain regions with afferents to the DR (Aghajanian and Wang, 1977; Lee et al., 2003; Peyron et al., 1998a; Vertes and Linley, 2008) and MR (Behzadi et al., 1990; Marcinkiewicz et al., 1989). However, such retrograde

tracing experiments do not provide information regarding cell-type-specific connectivity patterns but are appropriate for the mapping of major connections between brain regions (Köbbert et al., 2000). In essence, it is essential to identify the monosynaptic local and long-range inputs that target serotonergic neurons in order to generate an anatomical-functional understanding of the serotonin system.

Recently, the development of genetically modified rabies viruses for the transsynaptic tracing of inputs to a genetically defined neuron subtype (Wickersham et al., 2007) has allowed for characterization of local and long-range synaptic inputs onto defined neuron subtypes within a network (Miyamichi et al., 2013; Wall et al., 2013; Wall et al., 2010; Watabe-Uchida et al., 2012).

To identify the monosynaptic inputs that strictly target serotonergic neurons, we employed a genetic system enabling selective targeting of a modified rabies virus with monosynaptic retrograde tracing properties to serotonergic neurons located in the DR or MR. We analyzed connectivity with a whole-brain approach to resolve disputed circuits and to uncover previously unidentified circuits. We provide anatomical and functional evidence for the importance of direct synaptic inputs from prefrontal cortex (PFC) and lateral habenula (LH) in the regulation of serotonergic neurons. We further describe the presence of hyperdirect pathways from different levels of the basal ganglia circuit, including monosynaptic striatal inputs directly targeting serotonergic neurons.

RESULTS

Identification of Monosynaptic Inputs onto Serotonergic Neurons Using a Viral Tracing Strategy

We genetically targeted serotonergic neurons based on a transgenic mouse line expressing Cre recombinase in serotonergic neurons (Sert-Cre mice) (Zhuang et al., 2005). In Sert-Cre mice, we applied a genetically restricted two-virus approach to identify the whole-brain monosynaptic inputs onto serotonergic neurons located either in DR or MR. The strategy builds on targeting of Cre-dependent coexpression of the avian receptor TVA and the rabies glycoprotein G (RG) to serotonergic neurons, which is achieved through injection of AAV-DIO (Cardin et al., 2009) helper viruses (AAV-DIO-TVA-mCherry and AAV-DIO-RG; Figures 1A–1E) into DR or MR (Figure 1F) of Sert-Cre mice. The first injection is followed by delivery of a genetically modified rabies virus pseudotyped with the avian virus envelope protein (EnvA) (Figures 1A–1E). The rabies virus lacks the endogenous gene for RG and has been genetically modified to express the fluorescent protein EGFP (Figure 1B). As the rabies virus can only transduce cells expressing the TVA receptor, initial transduction and labeling is limited to Cre-expressing serotonergic neurons (Figure 1E). After retrograde transsynaptic labeling of input neurons, further spread of the rabies virus is inhibited due to the RG deletion (Figure 1E). In summary, the TVA receptor expression restricts the uptake of the EnvA-pseudotyped rabies virus specifically to serotonergic Cre-expressing neurons and the RG expression determines the strict monosynaptic spread.

We stereotaxically coinjected the helper viruses AAV-DIO-TVA-mCherry and AAV-DIO-RG into the DR or MR of adult Sert-Cre mice at day 1 (Figures 1C and 1D) and 21 days later the EnvA-coated Rabies-EGFP virus was injected at the same coordinates. Mice were perfused 1 week later, giving sufficient time for retrograde transsynaptic spread and prominent expression of EGFP in the input neurons. To define the specificity of our tracing approach, we performed a number of control experiments. First, we analyzed the expression specificity of the necessary tracing components. In Sert-Cre mice injected with AAV-DIO-TVA-mCherry and AAV-DIO-RG into either DR or MR, we found that expression of the TVA receptor was restricted to Cre-expressing cells (Figure 1G) and TVA-mCherry expression was restricted to serotonergic neurons (Figures 1H and 1I) (98.8% ± 2.1% TVA-mCherry positive neurons contained 5-HT, mean ± SD, n = 2,715 TVA-mCherry neurons, n = 3 mice). Furthermore, we determined that 95.4% ± 4.9% (mean ± SD, n = 2,236 5-HT-labeled neurons, n = 3 mice) of the serotonergic neurons were positive for TVA-mCherry and EGFP near the injection site, demonstrating a high degree of starter population targeting (Figures 1H and 1I).

To further determine the specificity of our approach, we applied the two-virus tracing strategy in DR of wild-type animals (i.e., Cre-negative). Whole-brain analysis revealed a very limited number of EGFP-expressing cells in control brains (64 ± 48 cells per mouse, mean ± SD, n = 4 mice), the majority localized near the injection site in DR (55 ± 44 cells, mean ± SD), representing approximately 0.1% of the transsynaptically labeled population in Sert-Cre tracing experiments (Figures S1A–S1D available online).

Automated Classification of Cell-Type-Specific Connectivity

To generate a whole-brain atlas of the EGFP-labeled input neurons, we imaged on average 50 coronal whole-brain sections per mouse spanning the entire forebrain, midbrain, and parts of hindbrain (Figures 2A–2C). Representative coronal images from transsynaptic tracing of inputs to serotonergic neurons in DR (Figure 2B) and in MR (Figure 2C) shows the whole-brain distribution of EGFP-labeled neurons (see also Movies S1, S2, S3, and S4).

To generate a comprehensive catalog with detailed account of the anatomical localization of each input neuron, we developed custom software to plot the EGFP-labeled neurons based on the Allen Institute mouse reference atlas (P56 mouse brain) containing 677 distinct anatomical regions. Imaged coronal brain sections were coregistered to the corresponding Allen Reference Atlas coordinate using nonrigid registration with free-form deformation (Rueckert et al., 1999) (Figure S2). The anatomical classification of EGFP-labeled neurons was determined by binary masks created from the Allen Mouse Reference Atlas, resulting in detection of labeled neurons in 553 out of the 677 discrete regions. Detailed images and anatomical definition can be accessed from an online resource (http://www.wholebrainsoftware.org). To evaluate the automatic classification system, we manually scored labeled neurons in regions with high-density labeling or sparse labeling and compared this to the automated result. This comparison demonstrated that the automatic classification slightly underestimated the number of labeled neurons, particularly in

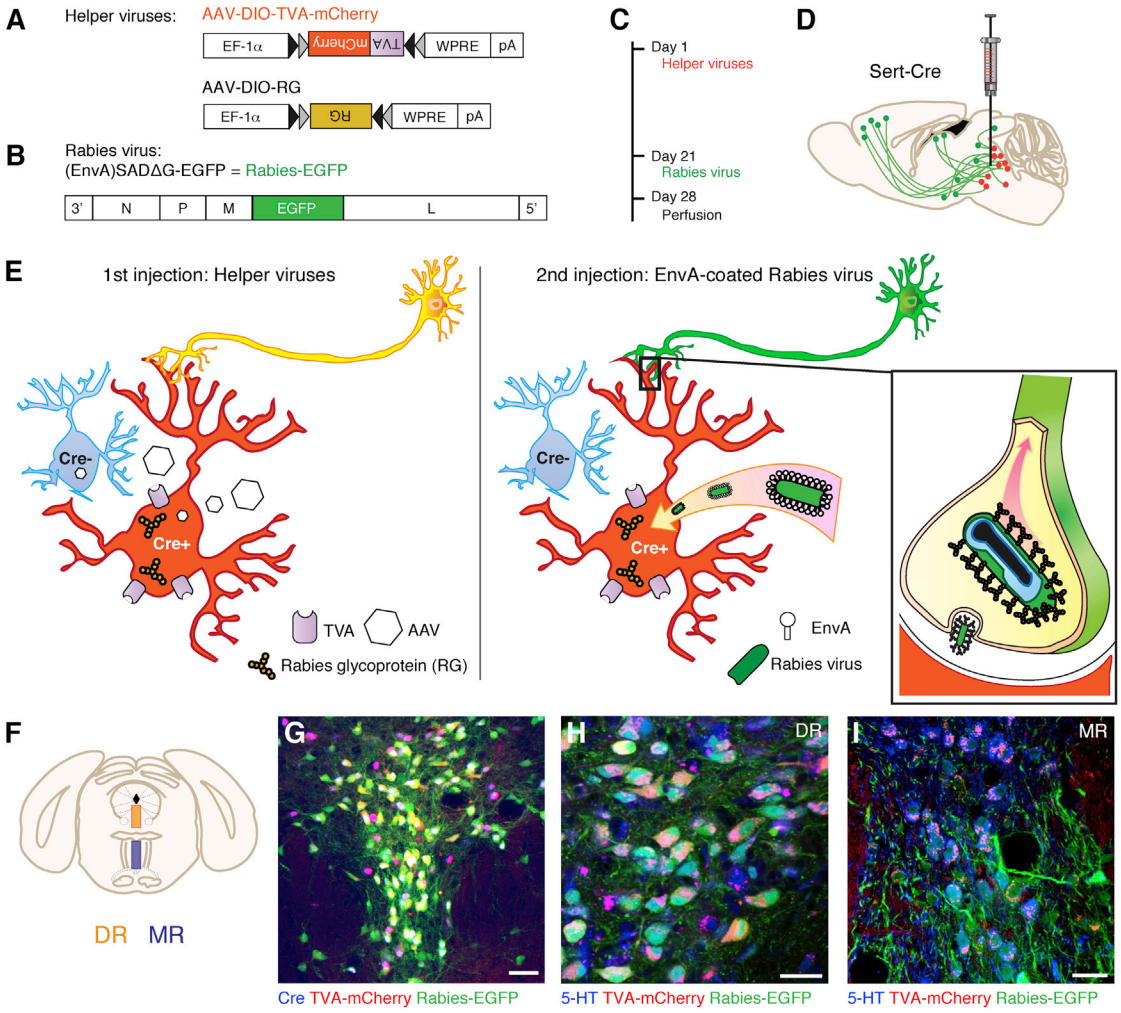

Figure 1. Experimental Strategy for Identification of Monosynaptic Inputs to Serotonergic Raphe Neurons

(A) AAV helper viruses with Cre-dependent expression of TVA receptor and RG.

(B) Genetically modified rabies virus is pseudotyped with EnvA. The RG gene is replaced by EGFP.

(C) Experimental timeline.

(D) Combination of the two-virus system and transgenic Sert-Cre-mice allows for brain-wide labeling of monosynaptic inputs (green) to serotonergic neurons (red) in DR or MR.

(E) The first injection (AAV helper viruses) induces selective expression of TVA and RG in Cre-expressing neurons (Cre+). The second injection (EnvA-coated rabies virus) results in rabies uptake by TVA-expressing neurons and transsynaptic retrograde transport of RG-coated rabies virus into upstream input neurons.

(F) Schematic of the anatomical localization of the midbrain dorsal raphe nucleus (DR; orange) and the median raphe nucleus (MR; purple).

(G) Cre-dependent targeting of serotonergic DR neurons in Sert-Cre mice. Cre recombinase (Cre; blue) induces expression of TVA-mCherry (red) and EGFP (green). Scale bar, 50 μm.

(H) DR serotonergic neurons (5-HT; blue) express TVA-mCherry (red) and EGFP (green) after viral injections in Sert-Cre mice. Scale bar, 30 μm.

(I) MR serotonergic neurons (5-HT; blue) express TVA-mCherry (red) and EGFP (green) after viral injections in Sert-Cre mice. Scale bar, 30 μm.

See also Figure S1.

densely labeled areas, but importantly did not result in any considerable false-positive detection (Figure S3). Automatic detection of labeled neurons allowed us to generate three-dimensional visualizations of the whole-brain inputs to serotonergic neurons in DR versus MR (Figures 3A–3K). We also defined the starting population (EGFP-labeled serotonergic neurons in DR or MR) based on anatomical distribution of the neurons (Figure 3L). As a measure of the efficacy in input detection, we calculated that the ratio of the input population to the starting population was 72× for monosynaptic tracing onto serotonergic neurons in DR and 29× for tracing inputs onto serotonergic neurons in MR (Figure 3M), indicating a comprehensive detection of inputs.

Statistical Inference on Whole-Brain Data

To analyze large-scale whole-brain data sets, we needed to confront the following issues: (1) the hierarchical nature and statistical dependency between nested anatomical regions, (2) the

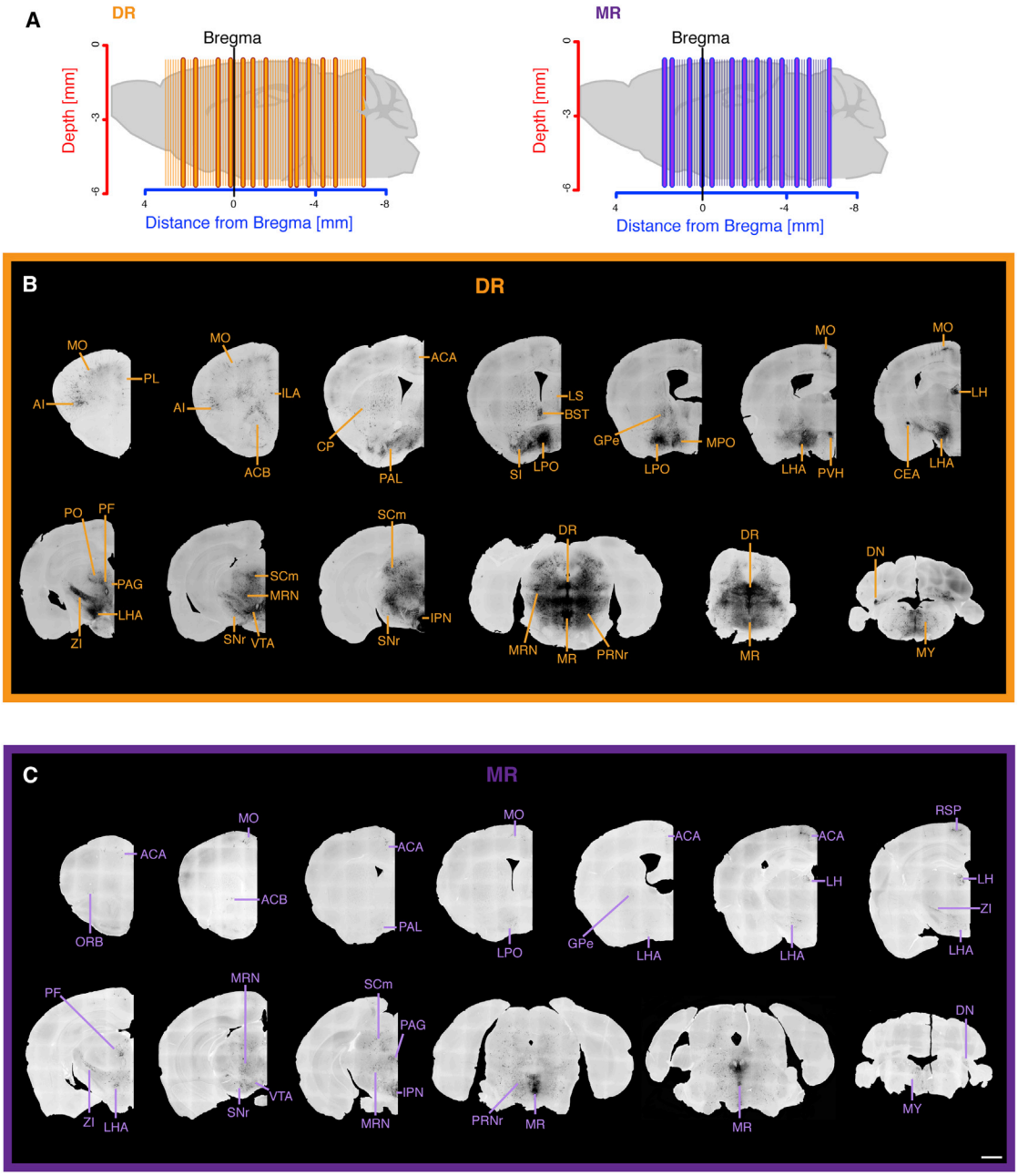

Figure 2. Anatomical Classification of Monosynaptic Inputs to Serotonergic Neurons in DR and MR

(A) Left: illustration of the anatomical localization of a subset (n = 13, thick vertical lines) of a total of 69 sections (thin vertical lines) from a representative animal with DR targeting (shown in B). Right: illustration of the anatomical localization of a subset (n = 13, thick vertical lines) of a total of 69 sections (thin vertical lines) from a representative animal with MR targeting (shown in C).

(B and C) Representative coronal sections showing labeling of monosynaptic input to serotonergic neurons in DR (B) or MR (C). For some sections only one hemisphere is shown. Scale bar, 1 mm.

Abbreviations used are the following: ACA, anterior cingulate area; ACB, nucleus accumbens; AI, agranular insular area; BST, bed nuclei of the stria terminalis; CEA, central amygdalar nucleus; CP, caudoputamen; DN, dentate nucleus; DR, dorsal raphe nucleus; GPe, globus pallidus, external segment; ILA, infralimbic area; IPN, interpeduncular nucleus; LH, lateral habenula; LHA, lateral hypothalamic area; LPO, lateral preoptic area; LS, lateral septal nucleus; MO, secondary motor area; MR, median raphe nucleus; MRN, midbrain reticular nucleus; MY, medulla; PAG, periaqueductal gray; PAL, pallidum; PF, parafascicular nucleus; PL, prelimbic area; PO, posterior complex of the thalamus; PPN, pedunculopontine nucleus; PRNr, pontine reticular nucleus; PVH, paraventricular hypothalamic nucleus; RSP, retrosplenial area; SCm, superior colliculus motor related; SNr, substantia nigra reticular part; VTA, ventral tegmental area; ZI, zona incerta. See also Figures S2 and S3.

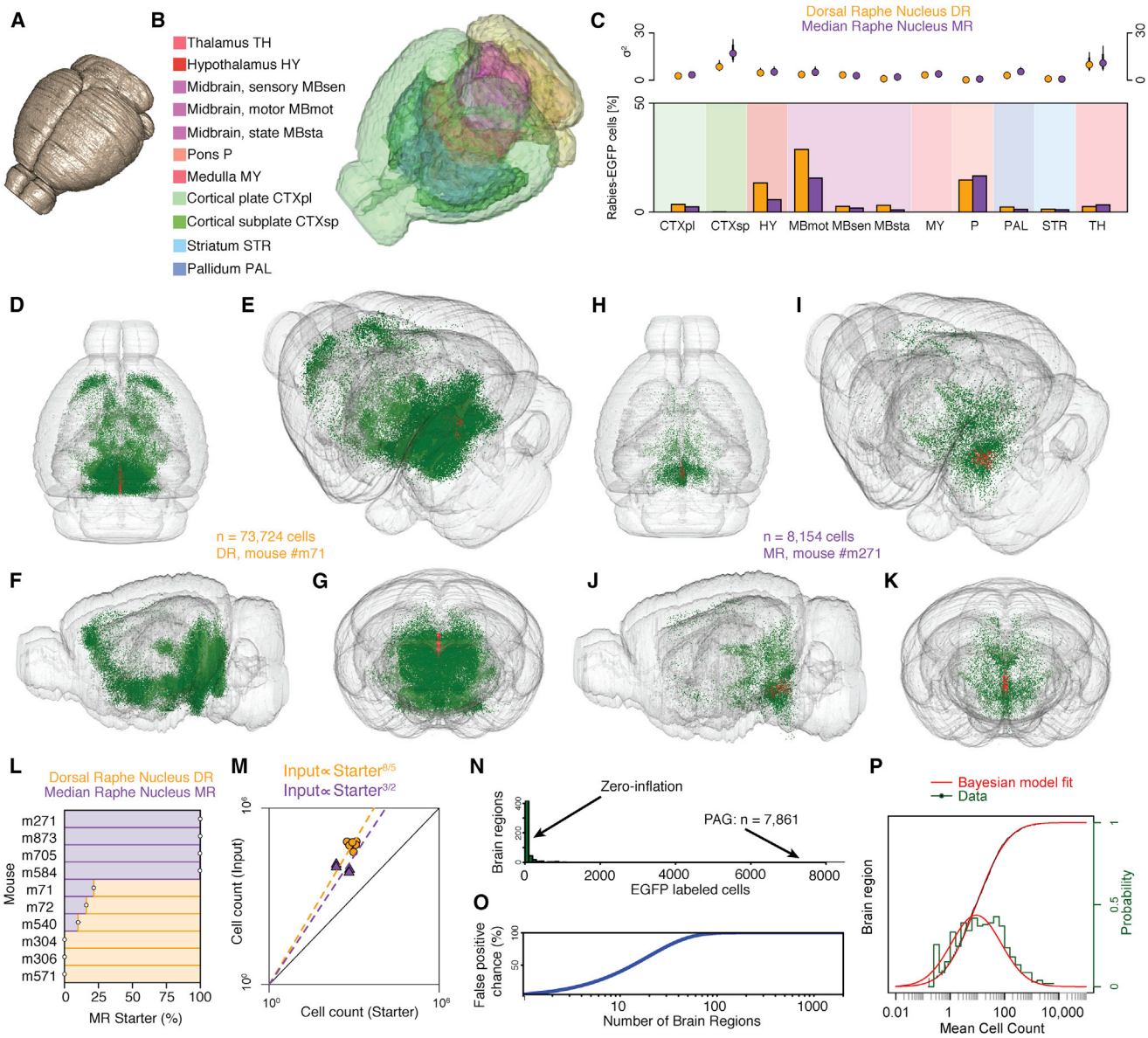

Figure 3. Three-Dimensional Mapping of All EGFP-Labeled Input Neurons in a Standardized Reference Atlas

(A) Isosurface reconstruction of the Allen Mouse Brain P56 Reference Atlas.

(B) Transparent isosurface of the mouse brain showing gross anatomical ontology.

(C) Between-mice variability in EGFP-labeling (σ^2) as a function of targeting and anatomical region (top). Percentage of EGFP-labeled cells in each gross anatomical region for tracing inputs onto serotonergic neurons in DR (orange) or MR (purple) (bottom).

(D–G) 3D visualization of whole-brain monosynaptic inputs to DR serotonergic neurons in one mouse showing 73,724 EGFP-labeled cells (green dots) from top (D), angle (E), side (F), and back (G) view. Red dots: starter population in DR (EGFP+/TVA-mCherry+).

(H–K) 3D visualization of whole-brain monosynaptic inputs to MR serotonergic neurons in one mouse showing 8,154 EGFP-labeled cells (green dots) from top (H), angle (I), side (J), and back (K) view. Red dots: starter population in MR (EGFP+/TVA-mCherry+).

(L) Specificity of DR versus MR targeting expressed as percentage of starter cells in MR.

(M) Relationship between number of starter (EGFP+/TVA-mCherry+) and input neurons (EGFP only).

(N) The distribution of EGFP-labeled cells among brain regions exhibits characteristics of a zero-inflated Poisson process.

(O) The problem of multiple comparisons: false-positive findings increase with the number of defined anatomical regions.

(P) Statistical Bayesian model fit (red) on the distribution of detected EGFP-labeled cells (density and cumulative density shown in the same graph.)

fact that most regions will exhibit little or no input at all (i.e., zero-inflation; Figure 3N), as well as (3) the problem of increasing chance of false-positive findings as number of brain regions tested increase (Bennett et al., 2009) (Figure 3O). To address these issues, we fitted a Bayesian hierarchical statistical model (Figure 3P) (Gelman, 2006). We first normalized the number of

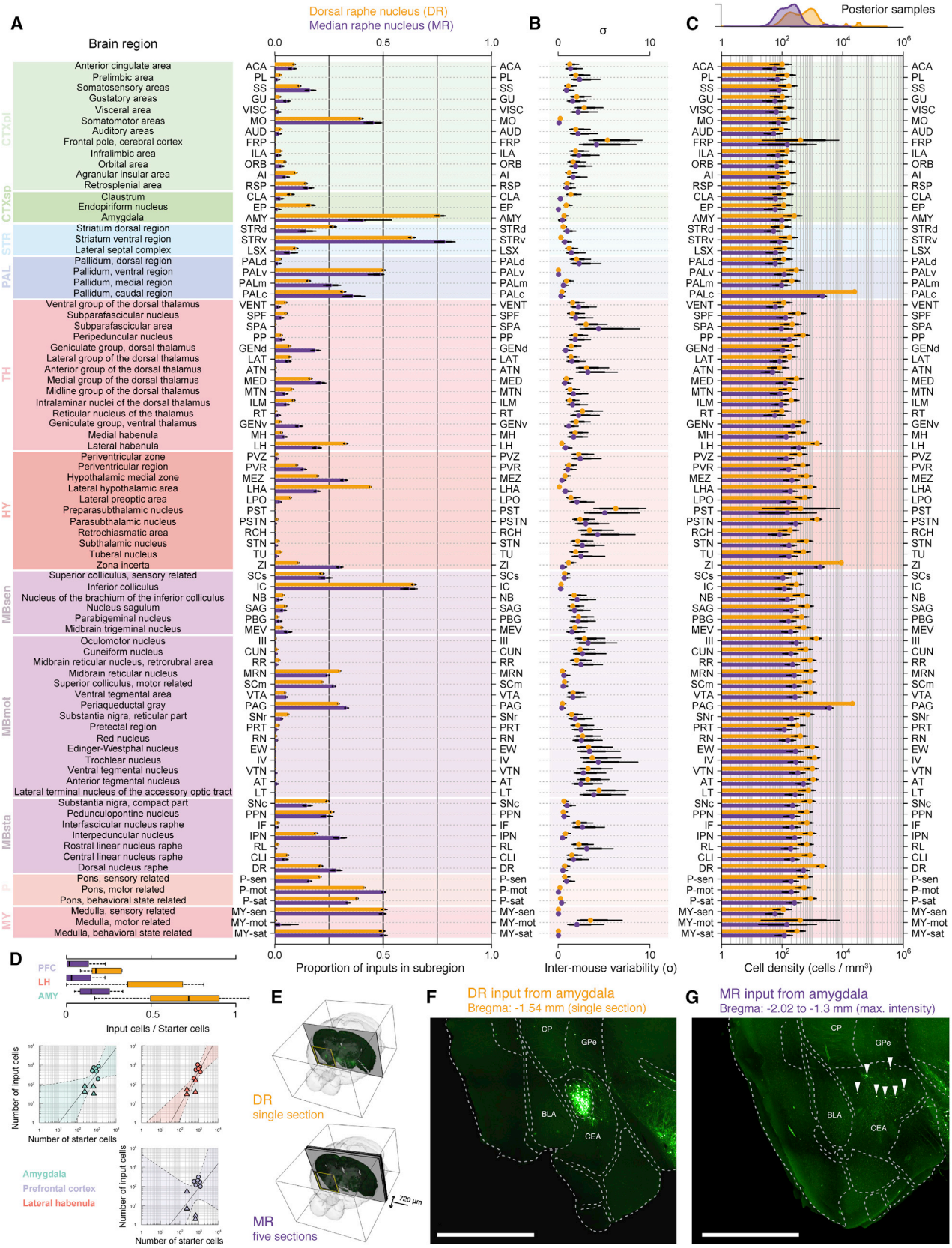

(legend on next page)

inputs in each brain region per the total number of inputs in each brain. We did this analysis in a hierarchical fashion where subregions were considered nested within larger brain regions such as midbrain, hypothalamus, and cortical regions. On average, there were more input neurons to DR (59,710 ± 15,759 neurons, mean ± SD, CV = 0.26) compared to MR (9,219 ± 2,481 neurons, mean ± SD, CV = 0.27). Conventional retrograde tracing studies have defined the main afferents to the DR region (Aghajanian and Wang, 1977; Lee et al., 2003; Peyron et al., 1998a; Vertes and Linley, 2008) and MR region (Behzadi et al., 1990; Marcinkiewicz et al., 1989). These studies have identified projections from LH, PFC, ventral posterior complex of the thalamus (VP), hypothalamic areas, including zona incerta (ZI), and central amygdala nucleus (CEA) as major inputs to the DR region. We identified 80 discrete anatomical areas that contained on average more than 100 EGFP-labeled neurons based on tracing of inputs to DR serotonergic neurons. We found that the anatomical areas containing most EGFP-labeled neurons were the periaqueductal gray (PAG), midbrain reticular nucleus (MRN), lateral hypothalamic area (LHA), pontine reticular nucleus (PRNr), motor-related superior colliculus (SCm), substantia nigra pars reticulata (SNr), ZI, ventral tegmental area (VTA), and inferior colliculus external (ICe). The larger absolute number of input neurons to serotonergic neurons in DR compared to the MR probably depends to some extent on the larger starting population in DR (DR starting population: 904 ± 251 neurons, mean ± SD, n = 6 mice) compared to MR (MR starting population: 457 ± 257 neurons, mean ± SD, n = 4 mice). Importantly, the difference in the total input population between DR and MR is almost 7-fold, but the starting population differs only by a factor of maximum two between DR and MR. As a result, comparing the proportion of input neurons by the total number of inputs will actually underestimate the difference in direct inputs to DR versus MR. It is therefore of importance to quantify the proportion of EGFP-labeled cells, as well as estimate the number of inputs as a function of the starting population. To estimate the effect on inputs per starter neuron, we fitted a zero-inflated Poisson regression model, which provided a good fit on the data (Figure 3P).

The whole-brain classification allowed us to perform statistical analysis on the anatomical specialization of the labeled input populations, by analyzing the distribution of EGFP-labeled neurons in specific subregions (i.e., orbital cortex [ORB]) as a function of the distribution within a larger anatomical region (i.e., cortical plate [CTXpl]), thereby generating a relative map of the preferential localization of projections from a larger brain area. We could then compute the proportion of the input population in discrete anatomical subregions targeting serotonergic neurons in DR versus MR (Figure 4A). We found that in basal ganglia regions such as the striatum (STR) and midbrain (MBmot, MBsta), there was a significant preference for input to serotonergic neurons to originate in ventral striatum (STRv), SNr, and pars compacta (SNc). EGFP-labeled neurons within hypothalamus (HY) displayed significant localization to LHA and LPO. The inputs that target serotonergic neurons in MR displayed preferential origin, for example, in the hypothalamic medial zone (MEZ), SCm, and ZI. We also determined the intermouse variability in the distribution of EGFP-labeled neurons per anatomical region to analyze potential labeling differences between animals or between tracing inputs to serotonergic neurons in DR versus MR. The intermouse variability measure showed that regions with extensive labeling displayed the lowest variability, arguing for an effect depending on the extent of rabies tracing efficacy rather than clear differences in circuit anatomy between mice (Figure 4B). We further determined the density of the EGFP-labeled input populations (EGFP-labeled neurons per defined anatomical volume; cells/mm^3; Figure 4C). This measure provided a qualitative identification of defined anatomical areas (e.g., PAG, LH, and ZI) that contain significant and densely labeled input populations (Figure 4C). The analysis focusing on the ratio between input and starter population allowed for detection of subtle but significant differences in EGFP labeling in defined anatomical subregions comparing DR and MR tracing (Figures 4E–4G). In summary, the brain-wide mapping of all EGFP-labeled input neurons allowed us to identify particular regions of interest for further characterization.

Whole-Brain Input Differences between DR and MR Serotonergic Neurons

The number of serotonergic neurons in DR is larger than in MR, although it is not established how that is represented in the absolute number or differential distribution of inputs. Conventional retrograde tracing studies to identify afferents to the DR region (Aghajanian and Wang, 1977; Lee et al., 2003; Peyron et al., 1998a; Vertes and Linley, 2008) and MR (Behzadi et al., 1990; Marcinkiewicz et al., 1989) have established the basic anatomy of inputs to these regions. MR afferents have been defined to mainly originate in hypothalamic structures such as lateral and dorsomedial hypothalamus, as well as medial PFC including anterior cingulate (ACA) and prelimbic cortex (PL). We found that serotonergic neurons in MR receive less pronounced inputs from PFC regions with a preference for afferents localized in

Figure 4. Comparative Whole-Brain Input Classification

(A) Proportion of EGFP-labeled cells for 81 nested anatomical subregions normalized against the total number of inputs in the given parent region (see Figure 3C).

(B) Variance component estimated for each anatomical subregion.

(C) EGFP-labeled cell density as a function of anatomical volume (cells/mm^3) for the same regions as in (A) and (B). Thick and thin lines display 80% and 95% Credible Intervals, respectively.

(D) Regions displaying greatest difference in ratio of input to starter neurons between DR (orange) and MR (purple), top. Number of inputs as a function of starter cells for the same regions, DR (circles) and MR (triangles).

(E) Visualization of the anatomical localization of coronal sections shown in (F; DR, single section) and (G; MR, five sections).

(F) Representative coronal section showing distribution of EGFP-labeled neurons in the amygdala complex after tracing serotonergic neurons in DR. Scale bar, 500 μm.

(G) Maximum intensity projection spanning 720 μm anterior-posterior showing sparse distribution of EGFP-labeled neurons in the amygdala complex after tracing serotonergic neurons in MR. Scale bar, 500 μm.

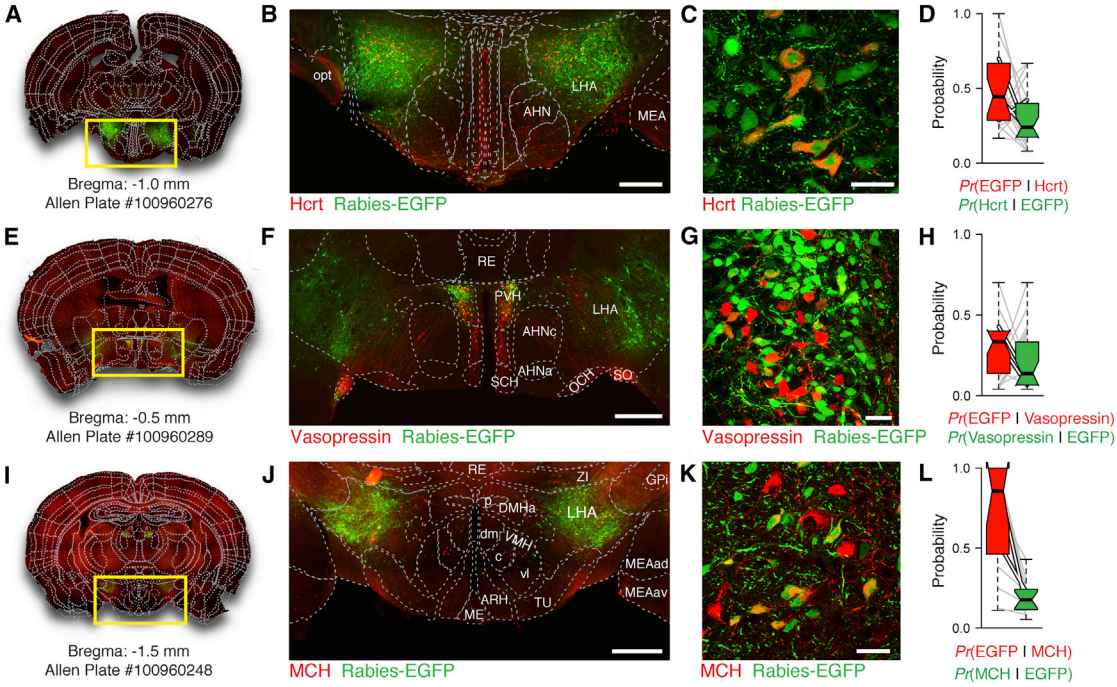

Figure 5. Cell-Type-Specific Hypothalamic Inputs onto Serotonergic Neurons

(A) Coronal whole-brain section with anatomical subdivisions at the level of LHA. Yellow rectangle defines image in (B).

(B) Hypocretin-expressing neurons in the LHA provide direct input to serotonergic neurons. Hcrt, red; Rabies-EGFP, green. Scale bar, 500 μm.

(C) A substantial proportion of input neurons (green) in LHA express Hcrt (red). Scale bar, 20 μm.

(D) Probability of EGFP+ given Hcrt+ (red) and of Hcrt+ given EGFP+ (green). Individual mice (thick white lines) and spatial subregions (thin gray lines). Median (thick black line), first and third quartile (box edges), and sample maximum and minimum (whiskers, dashed lines).

(E) Coronal whole-brain section with anatomical subdivisions at the level of PVHm. Yellow rectangle defines image in (F).

(F) Vasopressin-expressing neurons in the PVH provide direct input to serotonergic neurons. Vasopressin, red; Rabies-EGFP, green. Scale bar, 500 μm.

(G) A proportion of input neurons (green) in PVH express vasopressin (red). Scale bar, 20 μm.

(H) Probability of EGFP+ given Vasopressin+ (red) and of Vasopressin+ given EGFP+ (green). Individual mice (thick white lines) and spatial subregions (thin gray lines). Median (thick black line), first and third quartile (box edges), and sample maximum and minimum (whiskers, dashed lines).

(I) Coronal whole-brain section with anatomical subdivisions at the level of LHA. Yellow rectangle defines image in (J).

(J) MCH-expressing neurons in the LHA provide direct input to serotonergic neurons. MCH, red; Rabies-EGFP, green. Scale bar, 500 μm.

(K) A substantial proportion of input neurons (green) in LHA express MCH (red). Scale bar, 20 μm.

(L) Probability of EGFP+ given MCH+ (red) and of MCH+ given EGFP+ (green). Individual mice (thick white lines) and spatial subregions (thin gray lines). Median (thick black line), first and third quartile (box edges), and sample maximum and minimum (whiskers, dashed lines).

All abbreviations are according to the Allen mouse brain reference atlas. See also Figure S4.

hypothalamus and brainstem, for example ZI, MEZ, SCm, PAG, and pontine nuclei, compared to inputs targeting DR serotonergic neurons (Figures 4A–4C). Overall, the pattern of inputs targeting DR versus MR serotonergic neurons is similar on a gross anatomical level, although we find preferential distribution in anatomical subdivisions.

Direct Hypothalamic Inputs to Serotonergic Neurons

Hypothalamic nuclei are critical for homeostatic regulation of basic physiological processes including food intake, body temperature, and sleep-wake cycles (Saper, 2006). Hypothalamic subdivisions, such as LHA, have been implicated in sleep regulation through interaction with the serotonin system including projections to the DR (Celada et al., 2002; Peyron et al., 1998b), whereas, for example, the extent of DR-projecting neurons in tuberomammilary nucleus (TMN) has remained unclear (Lee et al., 2003; Peyron et al., 1998a). To resolve the contribution of defined hypothalamic cell types in terms of their inputs to serotonergic neurons, we analyzed the localization and identity of EGFP-labeled neurons in hypothalamus. We found substantial numbers of EGFP-labeled neurons in the LHA, TMN, and dorsomedial nucleus (DMH). Neurons containing hypocretin (Hcrt) project to DR (Lee et al., 2005; Peyron et al., 1998b) and hypocretin can modulate GABAergic as well as serotonergic neurons in DR (Liu et al., 2002). We found that Hcrt+ neurons in LHA provide a prominent monosynaptic input to DR serotonergic neurons (Figures 5A–5D; 21.7% ± 1.4% of EGFP-labeled cells express Hcrt, mean ± SD, n = 585 EGFP-labeled neurons, n = 3 mice). To define the identity of the other EGFP-labeled neurons in hypothalamus, we determined coexpression of input populations for vasopressin, melanin-concentrating hormone (MCH), oxytocin, and tyrosine hydroxylase (TH), identity markers that represent major hypothalamic populations. In the paraventricular hypothalamic nucleus, magnocellular division (PVHm), we observed a large number of

EGFP-labeled neurons, and a proportion of those expressed vasopressin (Figures 5E–5H; 10.5% ± 3.2% of EGFP-labeled neurons stained for vasopressin, mean ± SD, n = 457 EGFP-labeled neurons, n = 2 mice). We also found an EGFP-labeled population in LHA that was MCH positive (Figures 5I–5L; 17.6% ± 7.2% of the EGFP-labeled neurons in LHA stained for MCH, mean ± SD, n = 442 EGFP-labeled neurons, n = 2 mice). We further analyzed the intermouse variability in the colocalization of EGFP labeling and each identity marker (Figures 5D, 5H, and 5L). We found that out of the three populations (Hcrt, Vasopressin, and MCH), MCH-expressing neurons had the highest likelihood of showing monosynaptic inputs to serotonergic neurons (Figure 5L). In contrast, we found that EGFP-labeled neurons in LHA were negative for oxytocin and TH (Figure S4), demonstrating the complexity and specificity of cell-type-specific inputs from hypothalamic neurons onto serotonergic neurons.

Inputs from Amygdala

Conventional retrograde tracing studies have determined that projections from amygdala to DR originate primarily from the central nucleus (CEA), with limited inputs from the other amygdala nuclei (Peyron et al., 1998a; Retson and Van Bockstaele, 2013). In accordance with these studies, we detected the majority of EGFP-labeled amygdala input neurons in the CEA (mean 188 EGFP-labeled neurons per animal, n = 6 mice), and we found sparser distribution of EGFP-labeled neurons in basolateral amygdala (BLA) and medial amygdala nucleus (MEA). Interestingly, the amygdala complex showed the largest difference in connectivity pattern onto serotonergic neurons located in DR versus MR (Figures 4E–4G). We found that there was a preference for amygdala nuclei, in particular CEA, to have prominent monosynaptic inputs to serotonergic neurons in DR with very sparse connectivity with MR (Figures 4F and 4G). The extended amygdala circuit also includes the bed nuclei of stria terminalis (BST), which controls anxiety-related behaviors (Jennings et al., 2013; Kim et al., 2013). We found a dense and prominent projection from BST, particularly the anterior division, directly targeting DR serotonergic neurons (Figure 6C), which would be of interest to define functionally.

Inputs from Thalamus

Projections from DR preferentially target thalamic nuclei that are important for cognitive or emotional behaviors, in particular anterior nuclei, mediodorsal nucleus, and the midline and intralaminar nuclei, while avoiding principal nuclei (Vertes, 1991; Vertes et al., 2010). The thalamus itself is considered to have limited projections to DR and only from midline thalamus (paraventricular and paratenial nuclei) (Peyron et al., 1998a; Vertes and Linley, 2008). We found that thalamic nuclei with most EGFP-labeled neurons were the geniculate in ventral thalamus (GENv), paraventricular nucleus (PVT), medial part of mediodorsal nucleus (MDm), and the central part of mediodorsal nucleus (MDc). We also detected a large number of labeled neurons in parafascicular nucleus (PF), even though PF only receives moderate serotonergic inputs (Vertes et al., 2010).

Direct Prefrontal Cortex Inputs to Serotonergic Neurons

Several PFC regions have projections to DR (Gabbott et al., 2005; Gonçalves et al., 2009; Vertes, 2004), although the circuit organization or functional relevance of these pathways has not been established. Tracing of PFC inputs to the DR region using conventional retrograde approaches (Gabbott et al., 2005; Gonçalves et al., 2009; Hajós et al., 1998; Peyron et al., 1998a) have reported contradicting results concerning the anatomical distribution and density of input neurons. Importantly, the extent to which PFC projections monosynaptically target serotonergic neurons has been disputed, with the current view holding that most or all PFC glutamatergic afferents to DR target local inhibitory neurons, thereby resulting in disynaptic inhibition of serotonergic neurons (Hajós et al., 1998; Peyron et al., 1998a; Varga et al., 2001). Optogenetic stimulation of PFC efferents to the DR region results in behavioral changes associated with motivation and despair (Warden et al., 2012), although the impact on serotonergic neurons through monosynaptic or indirect pathways remains unknown. To determine the extent of monosynaptic inputs from PFC to serotonergic neurons, we first characterized the distribution of EGFP-labeled neurons in discrete frontal subdivisions. We found prominent labeling in PFC, with EGFP-labeled neurons located primarily in layer 5, including infralimbic (IL), prelimbic (PL), anterior cingulate (ACA), orbital, and insular cortex after tracing inputs to serotonergic neurons in DR (Figures 2B and 6A), with significantly fewer labeled neurons after MR tracing (Figure 2C). The tracing data therefore suggest a prominent and underappreciated role of discrete PFC networks in the direct regulation of serotonin. To further probe this hyperdirect pathway functionally, we analyzed the ACA to DR pathway using optogenetics and electrophysiology. We expressed ChR2 in ACA under a general promoter (AAV-CAG-ChR2-GFP) in Sert-Cre mice, in which we had genetically labeled serotonergic neurons with the fluorescent marker tdTomato (Figures 6E–6I; Figure S5). tdTomato-expressing neurons in DR expressed tryptophan hydroxylase (Tph), a specific marker for serotonergic neurons (97.3% ± 0.5% of tdTomato+ cells expressed Tph, mean ± SD, n = 230 cells, n = 3 mice), and displayed a distinct electrophysiological profile (Figure S6). We performed targeted whole-cell recordings from tdTomato-expressing serotonergic neurons together with optogenetic stimulation of afferents from ACA (Figure 6I). In agreement with the tracing data, we found monosynaptic responses in serotonergic neurons following optogenetic stimulation of axon terminals originating from ACA neurons (0.82 mV, mean; 2/5 serotonergic neurons showed clear ChR2-induced synaptic responses) and pharmacological application of an AMPA receptor antagonist (NBQX, 10μM) confirmed that the synaptic input was glutamatergic (Figure 6J). This hyperdirect excitatory PFC pathway provides for a direct excitatory control of serotonergic neurons that is most likely important for proper activity of the serotonin system.

Dense Direct Inputs from Lateral Habenula Control Serotonergic Neurons

The lateral habenula (LH) connects the basal ganglia to motivational and reward-related systems (Hong and Hikosaka, 2008) and has in particular been identified as a major projection system to DR based on conventional tracing (Aghajanian and Wang, 1977; Peyron et al., 1998a). The LH to DR projection is thought to primarily target and excite GABAergic neurons in DR, leading

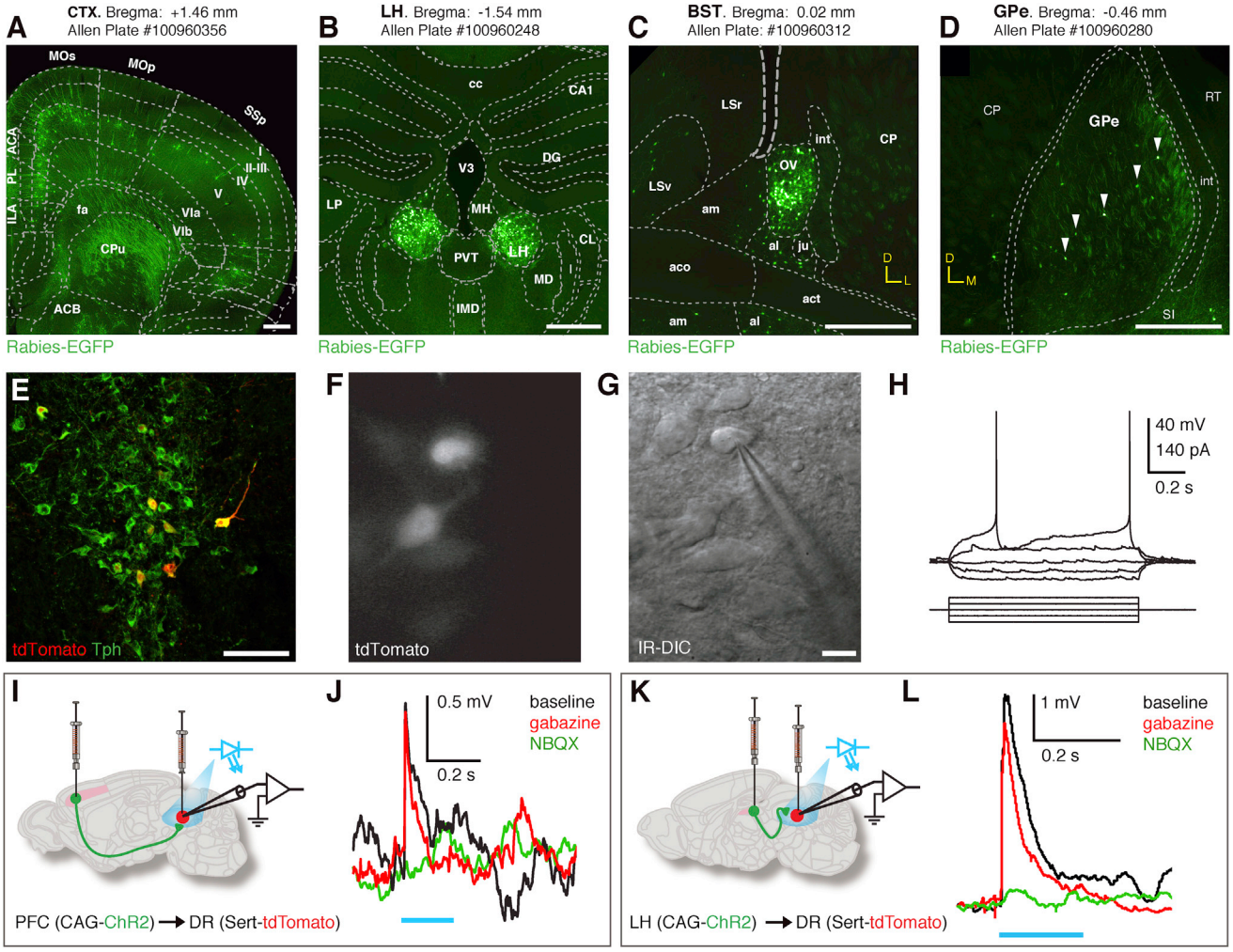

Figure 6. Hyperdirect Pathways Targeting Serotonergic Neurons

(A) EGFP-labeled neurons in PL and anterior ACA project directly to serotonergic neurons in DR. Scale bar, 300 μm.

(B) LH contains a dense population of EGFP-labeled neurons projecting directly to serotonergic neurons in DR. Scale bar, 300 μm.

(C) BST contains a dense population of EGFP-labeled neurons projecting directly to serotonergic neurons in DR. Scale bar, 300 μm.

(D) GPe contains EGFP-labeled neurons projecting directly to serotonergic neurons in DR. Scale bar, 300 μm. White arrowheads point to EGFP-labeled neurons.

(E) Genetically restricted tdTomato expression (red) in serotonergic neurons (Tph, green) after injections of the Cre-dependent AAV-FLEX-tdTomato virus into DR of Sert-Cre mice. Scale bar, 50 μm.

(F) Identification of DR serotonergic neurons (tdTomato-expressing, white) for targeted whole-cell recordings.

(G) Infrared differential interference contrast (IR-DIC) imaging of recorded serotonergic neuron (compare to F). Scale bar, 10 μm.

(H) Representative example of the electrophysiological profile of a serotonergic (tdTomato-expressing) neuron in response to step current injections.

(I) Optogenetic characterization of monosynaptic inputs from PFC to serotonergic neurons. Expression of ChR2-GFP (AAV-CAG-ChR2-GFP, green) in ACA neurons labels projections to DR. Serotonergic neurons labeled with tdTomato (AAV-FLEX-tdTomato, red). Blue light (465 nm, blue bar) activates ChR2. Targeted whole-cell recording of synaptic inputs in DR serotonergic neurons.

(J) Example of trace from a serotonergic neuron responding to optogenetic stimulation of PFC axon terminals (black trace). Synaptic response is blocked by NBQX (green trace) but not gabazine (red trace).

(K) Optogenetic characterization of monosynaptic inputs from LH to serotonergic neurons. Expression of ChR2-GFP (AAV-CAG-ChR2-GFP, green) in LH neurons labels projections to DR. Serotonergic neurons labeled with tdTomato (AAV-FLEX-tdTomato, red). Blue light (465 nm, blue bar) activates ChR2. Targeted whole-cell recording of synaptic inputs in DR serotonergic neurons.

(L) Example of trace from a serotonergic neuron responding to optogenetic stimulation of LH axon terminals (black trace). Synaptic response is blocked by NBQX (green trace) but not gabazine (red trace).

All abbreviations are according to the Allen mouse brain reference atlas.

See also Figures S5 and S6.

to inhibition of serotonergic neurons through a disynaptic pathway (Park, 1987; Varga et al., 2003). We found a dense and prominent labeling of LH neurons after tracing inputs onto serotonergic neurons in DR as well as MR (Figures 4D and 6B). The prominent labeling of LH neurons points to an important and underappreciated role of monosynaptic inputs from LH to serotonergic neurons. To functionally probe the hyperdirect LH pathway in the control of serotonergic neurons, we expressed ChR2 in LH neurons (AAV-CAG-ChR2-GFP) in Sert-Cre mice with tdTomato-labeled serotonergic neurons (Figure 6K; Figure S5). Optogenetic stimulation of ChR2-expressing LH neuron terminals in combination with whole-cell recordings from serotonergic neurons allowed us to functionally characterize the presence of monosynaptic inputs from LH. We found that photostimulation of the ChR2-expressing axon terminals resulted in rapid and pronounced depolarization of serotonergic neurons, demonstrating the monosynaptic nature of LH to serotonergic neurons (2.35 ± 1.8 mV, mean ± SD; 12/31 serotonergic neurons showed ChR2-induced monosynaptic responses). The majority of the ChR2-induced synaptic responses were blocked by an AMPA receptor antagonist (NBQX, 10 μM) but not by a GABA-A receptor antagonist (gabazine, 10 μM), confirming the strong and direct glutamatergic input onto serotonergic neurons from LH neurons (Figure 6L). We also found examples of strong ChR2-driven responses that were blocked by gabazine, although we could not conclude whether these represented monosynaptic or disynaptic responses (Figure S5). This hyperdirect pathway reinforces the importance of parallel circuits, with LH neurons providing a large and direct synaptic input to regulate serotonergic neuron activity.

Basal Ganglia Circuits Control Serotonergic Neurons

Basal ganglia circuits receive dense serotonergic inputs (Imai et al., 1986; Vertes and Linley, 2008). We identified a large number of EGFP-labeled neurons in several basal ganglia circuits, including STR, globus pallidus (GPe), and substantia nigra (SN) (Figure 2B). Projections from VTA and SNc to DR are considered to be mainly nondopaminergic, representing a GABAergic population (Kalén et al., 1988; Kirouac et al., 2004; Peyron et al., 1996; Vertes and Linley, 2008), although dopaminergic terminals are found in DR (Kitahama et al., 2000). We found widespread transsynaptic labeling of neurons in VTA and SNc after tracing from serotonergic neurons in DR and MR (Figure 7A). We found that a large proportion of the EGFP+ cells in medial VTA and SNc were negative for the dopaminergic marker tyrosine hydroxylase (TH). TH-expressing EGFP-labeled neurons were primarily concentrated to a ventrolateral part of the VTA bordering the SNc (57.1% ± 7.1% of EGFP-labeled neurons stained for TH, mean ± SD, n = 398 EGFP-labeled neurons, n = 3 mice), although we also found TH-positive EGFP-labeled neurons throughout SNc (43.7% ± 8.4% of EGFP-labeled neurons stained for TH, mean ± SD, n = 506 EGFP-labeled neurons, n = 3 mice) (Figures 7A and 7B). In agreement with our findings, the VTA contains a major GABAergic population that is considered to project to the DR region (Kirouac et al., 2004), probably corresponding to the EGFP-expressing nondopaminergic cells we have identified. Interestingly, we also identified a large number of EGFP-labeled neurons in SNr, the major output nucleus of the basal ganglia. The SNr has been found to primarily target specific thalamic nuclei but there are also nonthalamic projections described (Beckstead et al., 1979), which are thought to target the superior colliculus (SC) and the pedunculopontine nucleus (PPN) (Cebrián et al., 2005). The external segment of globus pallidus receives inputs from SN and striatum as well as from serotonergic neurons. We identified EGFP-labeled neurons in GPe along the whole rostrocaudal axis (Figure 6D) and distribution of labeled neurons was not restricted to the caudal pole of GPe, an area previously described to project to PAG (Shammah-Lagnado et al., 1996).

The striatum (caudoputamen [CP] and nucleus accumbens [ACB]) receives a wide serotonergic innervation, but it is not known whether striatal projection neurons could also provide a reciprocal input to serotonergic neurons. Interestingly, we found EGFP-labeled neurons in striatum after tracing inputs to DR serotonergic neurons, with preferential distribution of EGFP-labeled neurons in the ventral part (STRv), including prominent labeling of neurons in ACB (Figure 7C). The EGFP-labeled neurons displayed the characteristic morphology of striatal projection neurons, the medium spiny neurons (MSNs), including typical spiny dendrites (Figures 7D–7G). In addition, EGFP-labeled striatal neurons also expressed the MSN-specific marker FoxP1 (Tamura et al., 2004) (Figure 7D; 90.5% ± 1.4% of EGFP-labeled neurons were FoxP1+, mean ± SD, n = 190 neurons, n = 3 mice). MSNs can be further divided into D1-expressing MSNs projecting to nigra (striatonigral) and D2-expressing MSNs projecting mainly to globus pallidus (striatopallidal) (Gerfen et al., 1990). To define the MSN subtype that was transsynaptically labeled, we stained for the marker preproenkephalin (Penk), which identifies the D2-expressing MSN subtype (Curran and Watson, 1995). We found that most EGFP-labeled striatal neurons were negative for Penk (Figure 7E; 73.7% ± 20.6% EGFP-labeled neurons were Penk-negative, mean ± SD, n = 56 neurons, n = 3 mice), suggesting that D1-expressing MSNs constitute the major striatal input to serotonergic neurons. However, we could also demonstrate the presence of a subpopulation of EGFP-labeled MSNs that were positive for Penk (Figure 7F), indicating the existence of two parallel striatal projection pathways with monosynaptic inputs onto serotonergic neurons, pointing to the complexity of these circuits.

To directly address the function of the monosynaptic striatal projection onto serotonergic neurons, we performed optogenetic stimulation of genetically defined D1-expressing striatal projection neurons in combination with whole-cell recording from serotonergic neurons in DR (Figure 7H). Injection of a Cre-dependent viral vector (AAV-DIO-ChR2-mCherry) into the ventral striatum of D1-Cre mice (Gong et al., 2007) resulted in robust expression of ChR2-mCherry in striatal projection neurons including their axon terminals in close proximity to serotonergic neurons in DR (Figures S7A and S7B). We performed targeted whole-cell recordings of putative serotonergic neurons in DR as determined by their distinct electrophysiological profile, for example, their deep and wide after-hyperpolarization following a train of action potentials (Figure 7I; Figure S8). Photostimulation of ChR2-positive axon terminals originating from D1-expressing striatal neurons resulted in strong synaptic responses in serotonergic neurons (2.43 ± 1.1 mV, mean ± SD mV; 8/38 serotonergic neurons showed ChR2-induced monosynaptic responses). The

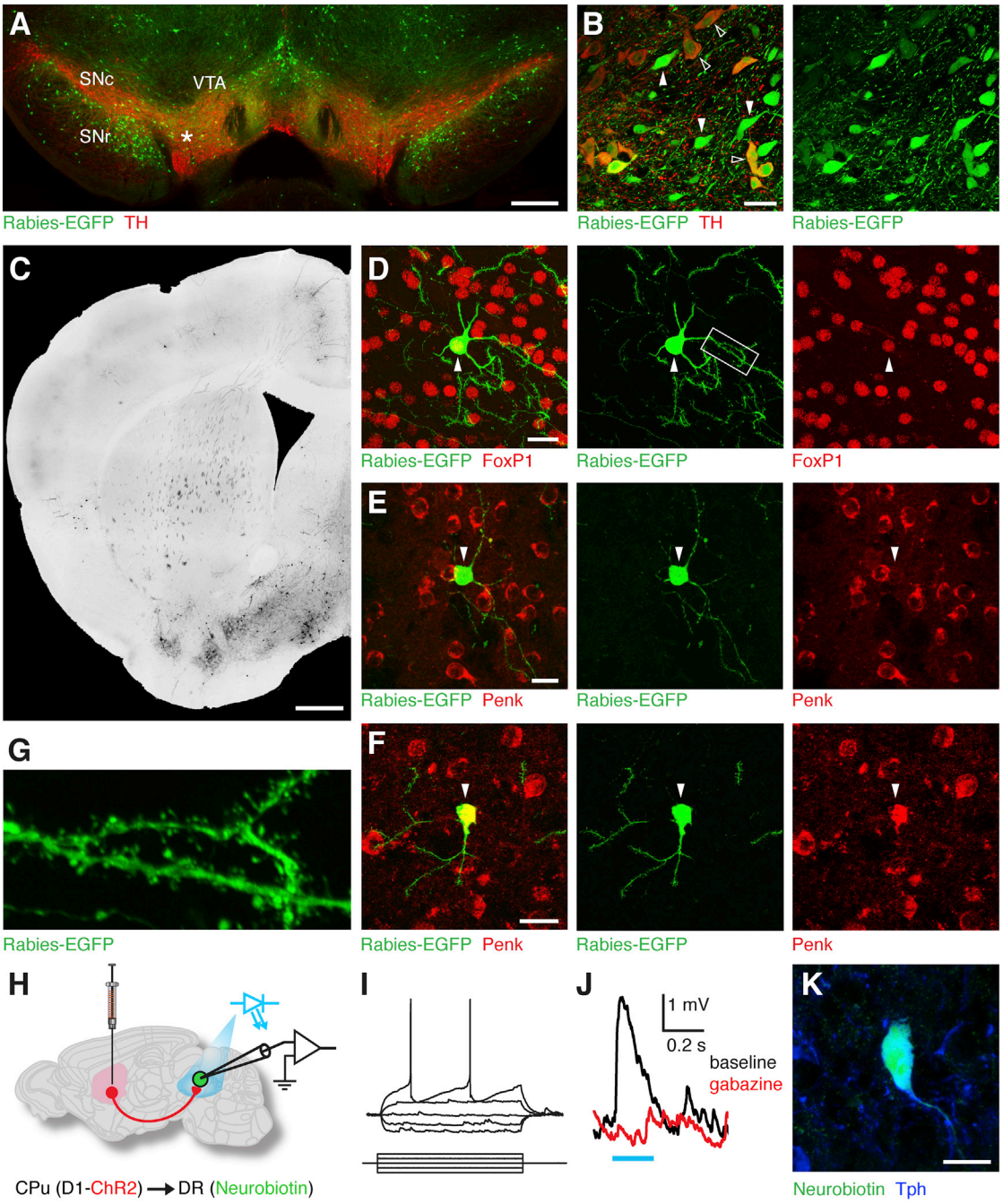

Figure 7. Hyperdirect Basal Ganglia Inputs to Serotonergic Neurons

(A) Representative coronal section of input labeling (EGFP, green) in VTA, SNc, and SNr to DR serotonergic neurons. The most abundant input is provided by the ventrolateral VTA (white asterisk). Scale bar, 500 μm.

(B) Both dopaminergic (EGFP+ [green]/TH$^+$ [red]; hollow arrowheads) and nondopaminergic neurons (EGFP+ [green]/TH− [red]; white arrowheads) in VTA, SNc, and SNr provide direct input to serotonergic raphe neurons. Scale bar, 30 μm.

(C) Representative coronal section at the level of striatum showing EGFP-labeled neurons (black). Scale bar, 500 μm.

(D) EGFP-labeled striatal neuron (green and arrowhead) expressing the MSN-specific transcription factor FoxP1 (red). White box denotes close-up of dendritic spines seen in (G). Scale bar, 20 μm.

(E) EGFP-labeled striatal neuron (green and arrowhead) lacking expression of the D2-specific marker Penk (red). Scale bar, 20 μm.

(F) EGFP-labeled striatal neuron (green and arrowhead) expressing the D2-specific marker Penk (red). Scale bar, 20 μm.

(G) Close-up of dendritic spines on the EGFP-labeled MSN neuron in (D) (white box in D).

(legend continued on next page)

light-induced synaptic responses were blocked by a GABA-A receptor antagonist (gabazine, 10 μM), demonstrating a direct GABAergic connection (Figure 7J; Figure S7G). We could further confirm the identity of the recorded putative serotonergic neurons displaying ChR2-driven synaptic responses by post hoc colabeling for neurobiotin and the serotonergic marker Tph (4 out of 8 responding cells confirmed Tph+; Figure 7K; Figures S7C–S7E).

In summary, we have identified a striatal projection pathway that monosynaptically controls serotonergic neurons in DR. This hyperdirect ventral striatal pathway can potentially represent a critical inhibitory feedback pathway onto serotonergic neurons. As a whole, our data reveal an unexpected diversity of parallel hyperdirect pathways from basal ganglia circuits that directly target serotonergic neurons, including pathways from distinct populations of the striatum, GPe, VTA, SNr, and SNc, as well as dopaminergic neurons located in the VTA/SNc region.

DISCUSSION

We present a comprehensive classification of whole-brain monosynaptic inputs that target serotonergic neurons in the DR and MR. Current understanding of input circuits to the DR or MR has been based on conventional retrograde tracing, which has technical limitations (Köbbert et al., 2000) and importantly does not allow for distinction of synaptic inputs to defined neuronal subtypes. Furthermore, conventional tracing has been associated with mapping of only small numbers of retrogradely labeled neurons (a few hundred), limiting detection to the major pathways. In contrast, we found that monosynaptic tracing of serotonergic neurons resulted in widespread and comprehensive labeling of their inputs, providing a detailed map of the circuits that can regulate serotonin. For example, our tracing of inputs onto DR serotonergic neurons mapped on average 59,710 neurons per animal on a standardized reference atlas, representing approximately a 72:1 ratio of total input to primary population ratio. This level of detail is essential to generate a quantitative and detailed map of whole-brain inputs to a specific neuron type. Transsynaptic tracing identified labeled neurons in the most anterior PFC areas, demonstrating that the tracing method did not exclude detection of long-range inputs. In summary, the large number of transsynaptically labeled neurons demonstrates the efficacy of the tracing strategy, and in particular the high density of labeled neurons in certain anatomical nuclei demonstrates the quantitative power of tracing synaptic connections. On the other hand, it is challenging to quantitatively define the comprehensiveness of rabies tracing approaches, since it remains unknown how transsynaptic spread of rabies virus is restricted or regulated by the structure or molecular profile of a synapse, including potential bias for active versus inactive synapses or the neurochemical identity of the synapse.

The transsynaptic tracing strategy allowed us to identify detailed quantitative as well as qualitative aspects of circuit organization. We have identified that serotonergic neurons receive prominent direct synaptic inputs from, for example, PFC and lateral habenula, regions that have previously been considered to target an intermediate inhibitory population in DR (Nakamura, 2013; Varga et al., 2001). In addition, we have found prominent inputs from different levels of basal ganglia circuits that control the serotonin system, a circuit organization that implicates a close interaction between the dopamine and serotonin system at several network levels. Importantly, we identified and functionally confirmed the presence of a hyperdirect pathway from striatum, of a striatal D1-expressing population that directly synapses onto serotonergic neurons in DR. Together, our data implicate a network for the integration of reward and motor behaviors based on basal ganglia and dopamine with the previously unappreciated synaptic control of serotonergic neurons, which in turn regulate basal ganglia function through their serotonin terminals. Our findings have however not yet resolved the functional significance of these hyperdirect pathways, particularly in light of postsynaptic integration with the parallel disynaptic pathways, which remains to be determined. Future computational models describing the role of serotonin for basal ganglia function (Reed et al., 2013) will benefit from identification of these parallel pathways to generate new hypotheses on network function during specific behaviors.

There are currently large efforts to determine brain connectivity at the macro- and mesoscale level by defining connectivity between regions (Oh et al., 2014; Zingg et al., 2014) as well as at the microscale level by electron microscopic reconstruction of small circuits (Denk et al., 2012), which in combination with the genetically defined analysis of neuron subtype-specific connectivity can reveal the organization of brain circuits. Whole-brain imaging using high-resolution light sheet microscopy or other advanced imaging methods will allow for the classification of cell-type-specific tracing, including integrity of axonal pathways and detailed neuronal morphology (Chung et al., 2013; Osten and Margrie, 2013).

Ultimately, knowledge of connectivity between genetically defined neuron types will be essential for modeling and understanding circuit function. Whole-brain mapping of connectivity patterns will be increasingly applied and development of tools that allow for automated high-throughput quantification and comparison between tracing studies will be critical. Imaging of neuronal activity through rabies-restricted expression of calcium-sensitive or voltage-sensitive proteins in presynaptic

(H) Optogenetic characterization of monosynaptic inputs from D1-expressing striatal projection neurons on serotonergic neurons. Expression of ChR2-mCherry (AAV-DIO-ChR2-mCherry, red) in D1+ striatal neurons labels projections to DR. Blue light (465 nm, blue bar) activates ChR2. Synaptic responses in serotonergic neurons are recorded using whole-cell recording.
(I) Characterization of electrophysiological properties of recorded neurons in DR identifies them as serotonergic.
(J) Example of monosynaptic response (black trace) in a serotonergic DR neuron after optogenetic stimulation of D1+ striatal projection terminals. The synaptic response is blocked by gabazine (red trace), demonstrating a direct GABAergic synapse.
(K) Confirmation of serotonergic identity of recorded DR neuron by post hoc immunostaining for Neurobiotin (green) and Tph (blue). Scale bar, 20 μm.
See also Figures S7 and S8.

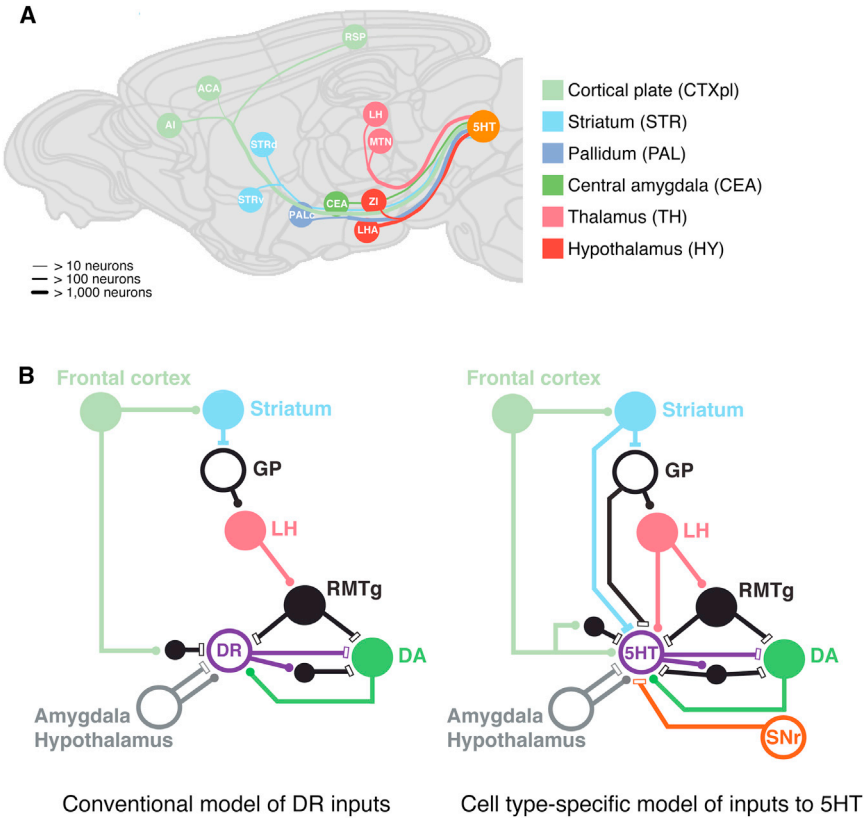

Figure 8. Whole-Brain Model and Hyperdirect Circuitry of Monosynaptic Inputs onto Serotonergic Neurons

(A) A whole-brain model of selected prominent monosynaptic inputs onto serotonergic neurons. Inputs shown onto serotonergic neurons (5-HT) from isocortex (ACA, AI, RSP), striatum (STRd, STRv), caudal pallidum (PALc), thalamus (LH, MTN), central amygdala nucleus (CEA), and hypothalamus (LHA, ZI). Line thickness represents input numbers.

(B) An updated circuitry model based on the cell-type-specific inputs to serotonergic neurons (5-HT). Conventional model adapted from Nakamura (2013). Excitatory inputs depicted with circles, inhibitory inputs with rectangles.

Color scheme is based on the Allen reference mouse brain atlas.

populations as well as optogenetic manipulation of their activity can lead toward identifying their behavioral impact. Such approaches will depend on the development of genetically improved rabies virus strains with reduced neuronal toxicity, to allow for long-term in vivo imaging and optogenetic experiments. In addition, the development of efficient anterograde monosynaptic tracing systems will be important for identifying the downstream targets of a particular neuron type (Beier et al., 2011; Lo and Anderson, 2011).

Based on this whole-brain mapping, we propose a revised model of brain circuits that target serotonergic neurons. This model emphasizes the importance of hyperdirect pathways from PFC, LH, STR, GPe, SNr, SNc, and VTA (Figure 8).

The identification of the distinct local and long-range synaptic inputs onto serotonergic neurons opens up for the possibility for further subtype-specific classification of such populations based on discovery of molecular markers, using, for example, RNA sequencing, which in turn is the basis for generating new types of genetic and functional manipulations of candidate input populations.

EXPERIMENTAL PROCEDURES

AAV Cloning

TVA, mCherry, and RG were amplified from pCMMP-TVA800 (Wickersham et al., 2007) (Addgene plasmid 15778), pAAV-EF1a-double-floxed-hChR2(H134R)-mCherry-WPRE-HGHpA (Addgene plasmid 20297), and pHCMV-Rabies G (Sena-Esteves et al., 2004) (Addgene plasmid 15785). Details can be found in the Supplemental Experimental Procedures.

Rabies Virus Production

The EnvA-pseudotyped rabies virus (EnvA)-SADΔG-EGFP (referred to as Rabies-EGFP) was produced according to a published protocol (Wickersham et al., 2010).

Virus Injections

Animal experiments were carried out following guidelines of the Stockholm municipal committee. Sert-Cre mice (Zhuang et al., 2005) aged 2–7 months were used for monosynaptic tracing. A volume of 0.5 μl (MR injections) or 0.8 μl (DR injections) containing equal amounts of AAV-DIO-TVA-mCherry (1.5×10^{-13} particles/ml) and AAV-DIO-RG (1.5×10^{-13} particles/ml) was injected with a 25° angle for DR (coordinates in mm: AP −4.5, L 1.35, V −3.1) and with a 30° angle for MR (coordinates in mm: AP −4.3, L 2.6, V −5.0). Twenty-one days later, 1 μl of EnvA-coated Rabies-EGFP virus (3.03×10^{-9} particles/ml) was injected into the same site. Details on virus injections can be found in the Supplemental Experimental Procedures.

Histology and Automated Anatomical Classification

Coronal sections (60 μm) were cut using a vibratome (Leica VT1000, Leica Microsystems). Brain sections for whole-brain mapping were imaged with a 10× objective (NA: 0.4) on a Leica DM6000B fluorescent microscope with a Hamamatsu Orca-FLASH 4.0 digital camera at 16 bit depth resolution. Segmentation of cell bodies and registration of position on the Allen mouse reference atlas was performed using custom software (see Supplemental Experimental Procedures).

SUPPLEMENTAL INFORMATION

Supplemental Information includes Supplemental Experimental Procedures, eight figures, and four movies and can be found with this article online at http://dx.doi.org/10.1016/j.neuron.2014.07.002.

ACKNOWLEDGMENTS

We thank Tomas Hökfelt for antibodies, valuable support, and advice, Christian Broberger and Arash Hellysaz for antibodies and advice on hypothalamic circuits, and Victor Salander and Joseph Bergenstråhle for technical assistance. We thank Ed Callaway, Ian Wickersham, and Klaus Conzelmann for reagents for virus cloning and virus production. We thank Karl Deisseroth and Ed Boyden for viral constructs. This work was supported by grants to K.M. from the Swedish Brain Foundation (Hjärnfonden), the Karolinska Institutet Strategic Research program in Neuroscience (StratNeuro), the Magnus Bergvall

Stiftelse, and the Åke Wibergs Stiftelse. G.S. was supported by StratNeuro and an ERC Starting Grant. M.C. was supported by the Swedish Research Council. K.M. was supported by a grant from the Williams K. Bowes Jr. Foundation.

Accepted: June 26, 2014
Published: August 6, 2014

REFERENCES

Abi-Dargham, A., Laruelle, M., Aghajanian, G.K., Charney, D., and Krystal, J. (1997). The role of serotonin in the pathophysiology and treatment of schizophrenia. J. Neuropsychiatry Clin. Neurosci. *9*, 1–17.

Abrams, J.K., Johnson, P.L., Hollis, J.H., and Lowry, C.A. (2004). Anatomic and functional topography of the dorsal raphe nucleus. Ann. N Y Acad. Sci. *1018*, 46–57.

Aghajanian, G.K., and Wang, R.Y. (1977). Habenular and other midbrain raphe afferents demonstrated by a modified retrograde tracing technique. Brain Res. *122*, 229–242.

Azmitia, E.C., and Segal, M. (1978). An autoradiographic analysis of the differential ascending projections of the dorsal and median raphe nuclei in the rat. J. Comp. Neurol. *179*, 641–667.

Beckstead, R.M., Domesick, V.B., and Nauta, W.J. (1979). Efferent connections of the substantia nigra and ventral tegmental area in the rat. Brain Res. *175*, 191–217.

Behzadi, G., Kalén, P., Parvopassu, F., and Wiklund, L. (1990). Afferents to the median raphe nucleus of the rat: retrograde cholera toxin and wheat germ conjugated horseradish peroxidase tracing, and selective D-[3H]aspartate labelling of possible excitatory amino acid inputs. Neuroscience *37*, 77–100.

Beier, K.T., Saunders, A., Oldenburg, I.A., Miyamichi, K., Akhtar, N., Luo, L., Whelan, S.P., Sabatini, B., and Cepko, C.L. (2011). Anterograde or retrograde transsynaptic labeling of CNS neurons with vesicular stomatitis virus vectors. Proc. Natl. Acad. Sci. USA *108*, 15414–15419.

Bennett, C.M., Wolford, G.L., and Miller, M.B. (2009). The principled control of false positives in neuroimaging. Soc. Cogn. Affect. Neurosci. *4*, 417–422.

Cardin, J.A., Carlén, M., Meletis, K., Knoblich, U., Zhang, F., Deisseroth, K., Tsai, L.H., and Moore, C.I. (2009). Driving fast-spiking cells induces gamma rhythm and controls sensory responses. Nature *459*, 663–667.

Cebrián, C., Parent, A., and Prensa, L. (2005). Patterns of axonal branching of neurons of the substantia nigra pars reticulata and pars lateralis in the rat. J. Comp. Neurol. *492*, 349–369.

Celada, P., Casanovas, J.M., Paez, X., and Artigas, F. (2002). Control of serotonergic neurons in the dorsal raphe nucleus by the lateral hypothalamus. Brain Res. *932*, 79–90.

Chung, K., Wallace, J., Kim, S.Y., Kalyanasundaram, S., Andalman, A.S., Davidson, T.J., Mirzabekov, J.J., Zalocusky, K.A., Mattis, J., Denisin, A.K., et al. (2013). Structural and molecular interrogation of intact biological systems. Nature *497*, 332–337.

Clarke, H.F., Dalley, J.W., Crofts, H.S., Robbins, T.W., and Roberts, A.C. (2004). Cognitive inflexibility after prefrontal serotonin depletion. Science *304*, 878–880.

Cools, R., Roberts, A.C., and Robbins, T.W. (2008). Serotoninergic regulation of emotional and behavioural control processes. Trends Cogn. Sci. *12*, 31–40.

Curran, E.J., and Watson, S.J., Jr. (1995). Dopamine receptor mRNA expression patterns by opioid peptide cells in the nucleus accumbens of the rat: a double in situ hybridization study. J. Comp. Neurol. *361*, 57–76.

Dahlstroem, A., and Fuxe, K. (1964). Evidence for the existence of monoamine-containing neurons in the central nervous system. I. Demonstration of monoamines in the cell bodies of brain stem neurons. Acta Physiol. Scand. Suppl. *232*, 1–55.

Dayan, P., and Huys, Q.J. (2009). Serotonin in affective control. Annu. Rev. Neurosci. *32*, 95–126.

Denk, W., Briggman, K.L., and Helmstaedter, M. (2012). Structural neurobiology: missing link to a mechanistic understanding of neural computation. Nat. Rev. Neurosci. *13*, 351–358.

Descarries, L., Watkins, K.C., Garcia, S., and Beaudet, A. (1982). The serotonin neurons in nucleus raphe dorsalis of adult rat: a light and electron microscope radioautographic study. J. Comp. Neurol. *207*, 239–254.

Fu, W., Le Maître, E., Fabre, V., Bernard, J.F., David Xu, Z.Q., and Hökfelt, T. (2010). Chemical neuroanatomy of the dorsal raphe nucleus and adjacent structures of the mouse brain. J. Comp. Neurol. *518*, 3464–3494.

Fuxe, K. (1965). Evidence for the existence of monoamine neurons in the central nervous system. IV. Distribution of monoamine nerve terminals in the central nervous system. Acta Physiol. Scand. Suppl. *247*, 247, 37.

Gabbott, P.L., Warner, T.A., Jays, P.R., Salway, P., and Busby, S.J. (2005). Prefrontal cortex in the rat: projections to subcortical autonomic, motor, and limbic centers. J. Comp. Neurol. *492*, 145–177.

Gelman, A. (2006). Multilevel (hierarchical) modeling: what it can and cannot do. Technometrics *48*, 432–435.

Gerfen, C.R., Engber, T.M., Mahan, L.C., Susel, Z., Chase, T.N., Monsma, F.J., Jr., and Sibley, D.R. (1990). D1 and D2 dopamine receptor-regulated gene expression of striatonigral and striatopallidal neurons. Science *250*, 1429–1432.

Gonçalves, L., Nogueira, M.I., Shammah-Lagnado, S.J., and Metzger, M. (2009). Prefrontal afferents to the dorsal raphe nucleus in the rat. Brain Res. Bull. *78*, 240–247.

Gong, S., Doughty, M., Harbaugh, C.R., Cummins, A., Hatten, M.E., Heintz, N., and Gerfen, C.R. (2007). Targeting Cre recombinase to specific neuron populations with bacterial artificial chromosome constructs. J. Neurosci. *27*, 9817–9823.

Hajós, M., Richards, C.D., Székely, A.D., and Sharp, T. (1998). An electrophysiological and neuroanatomical study of the medial prefrontal cortical projection to the midbrain raphe nuclei in the rat. Neuroscience *87*, 95–108.

Hale, M.W., and Lowry, C.A. (2011). Functional topography of midbrain and pontine serotonergic systems: implications for synaptic regulation of serotonergic circuits. Psychopharmacology (Berl.) *213*, 243–264.

Homberg, J.R. (2012). Serotonin and decision making processes. Neurosci. Biobehav. Rev. *36*, 218–236.

Hong, S., and Hikosaka, O. (2008). The globus pallidus sends reward-related signals to the lateral habenula. Neuron *60*, 720–729.

Huot, P., Fox, S.H., and Brotchie, J.M. (2011). The serotonergic system in Parkinson's disease. Prog. Neurobiol. *95*, 163–212.

Imai, H., Steindler, D.A., and Kitai, S.T. (1986). The organization of divergent axonal projections from the midbrain raphe nuclei in the rat. J. Comp. Neurol. *243*, 363–380.

Jacobs, B.L., and Azmitia, E.C. (1992). Structure and function of the brain serotonin system. Physiol. Rev. *72*, 165–229.

Jennings, J.H., Sparta, D.R., Stamatakis, A.M., Ung, R.L., Pleil, K.E., Kash, T.L., and Stuber, G.D. (2013). Distinct extended amygdala circuits for divergent motivational states. Nature *496*, 224–228.

Kalén, P., Skagerberg, G., and Lindvall, O. (1988). Projections from the ventral tegmental area and mesencephalic raphe to the dorsal raphe nucleus in the rat. Evidence for a minor dopaminergic component. Exp. Brain Res. *73*, 69–77.

Kim, S.Y., Adhikari, A., Lee, S.Y., Marshel, J.H., Kim, C.K., Mallory, C.S., Lo, M., Pak, S., Mattis, J., Lim, B.K., et al. (2013). Diverging neural pathways assemble a behavioural state from separable features in anxiety. Nature *496*, 219–223.

Kirby, L.G., Pernar, L., Valentino, R.J., and Beck, S.G. (2003). Distinguishing characteristics of serotonin and non-serotonin-containing cells in the dorsal raphe nucleus: electrophysiological and immunohistochemical studies. Neuroscience *116*, 669–683.

Kirouac, G.J., Li, S., and Mabrouk, G. (2004). GABAergic projection from the ventral tegmental area and substantia nigra to the periaqueductal gray region and the dorsal raphe nucleus. J. Comp. Neurol. *469*, 170–184.

Kitahama, K., Nagatsu, I., Geffard, M., and Maeda, T. (2000). Distribution of dopamine-immunoreactive fibers in the rat brainstem. J. Chem. Neuroanat. *18*, 1–9.

Köbbert, C., Apps, R., Bechmann, I., Lanciego, J.L., Mey, J., and Thanos, S. (2000). Current concepts in neuroanatomical tracing. Prog. Neurobiol. *62*, 327–351.

Lee, H.S., Kim, M.A., Valentino, R.J., and Waterhouse, B.D. (2003). Glutamatergic afferent projections to the dorsal raphe nucleus of the rat. Brain Res. *963*, 57–71.

Lee, H.S., Park, S.H., Song, W.C., and Waterhouse, B.D. (2005). Retrograde study of hypocretin-1 (orexin-A) projections to subdivisions of the dorsal raphe nucleus in the rat. Brain Res. *1059*, 35–45.

Liu, R.J., van den Pol, A.N., and Aghajanian, G.K. (2002). Hypocretins (orexins) regulate serotonin neurons in the dorsal raphe nucleus by excitatory direct and inhibitory indirect actions. J. Neurosci. *22*, 9453–9464.

Lo, L., and Anderson, D.J. (2011). A Cre-dependent, anterograde transsynaptic viral tracer for mapping output pathways of genetically marked neurons. Neuron *72*, 938–950.

Lucki, I. (1998). The spectrum of behaviors influenced by serotonin. Biol. Psychiatry *44*, 151–162.

Marcinkiewicz, M., Morcos, R., and Chrétien, M. (1989). CNS connections with the median raphe nucleus: retrograde tracing with WGA-apoHRP-Gold complex in the rat. J. Comp. Neurol. *289*, 11–35.

Miyamichi, K., Shlomai-Fuchs, Y., Shu, M., Weissbourd, B.C., Luo, L., and Mizrahi, A. (2013). Dissecting local circuits: parvalbumin interneurons underlie broad feedback control of olfactory bulb output. Neuron *80*, 1232–1245.

Nakamura, K. (2013). The role of the dorsal raphé nucleus in reward-seeking behavior. Front. Integr. Neurosci. *7*, 60.

Ochi, J., and Shimizu, K. (1978). Occurrence of dopamine-containing neurons in the midbrain raphe nuclei of the rat. Neurosci. Lett. *8*, 317–320.

Oh, S.W., Harris, J.A., Ng, L., Winslow, B., Cain, N., Mihalas, S., Wang, Q., Lau, C., Kuan, L., Henry, A.M., et al. (2014). A mesoscale connectome of the mouse brain. Nature *508*, 207–214.

Osten, P., and Margrie, T.W. (2013). Mapping brain circuitry with a light microscope. Nat. Methods *10*, 515–523.

Park, M.R. (1987). Monosynaptic inhibitory postsynaptic potentials from lateral habenula recorded in dorsal raphe neurons. Brain Res. Bull. *19*, 581–586.

Paul, E.D., and Lowry, C.A. (2013). Functional topography of serotonergic systems supports the Deakin/Graeff hypothesis of anxiety and affective disorders. J. Psychopharmacol. (Oxford) *27*, 1090–1106.

Peyron, C., Luppi, P.H., Fort, P., Rampon, C., and Jouvet, M. (1996). Lower brainstem catecholamine afferents to the rat dorsal raphe nucleus. J. Comp. Neurol. *364*, 402–413.

Peyron, C., Petit, J.M., Rampon, C., Jouvet, M., and Luppi, P.H. (1998a). Forebrain afferents to the rat dorsal raphe nucleus demonstrated by retrograde and anterograde tracing methods. Neuroscience *82*, 443–468.

Peyron, C., Tighe, D.K., van den Pol, A.N., de Lecea, L., Heller, H.C., Sutcliffe, J.G., and Kilduff, T.S. (1998b). Neurons containing hypocretin (orexin) project to multiple neuronal systems. J. Neurosci. *18*, 9996–10015.

Ranade, S.P., and Mainen, Z.F. (2009). Transient firing of dorsal raphe neurons encodes diverse and specific sensory, motor, and reward events. J. Neurophysiol. *102*, 3026–3037.

Reed, M.C., Nijhout, H.F., and Best, J. (2013). Computational studies of the role of serotonin in the basal ganglia. Front. Integr. Neurosci. *7*, 41.

Retson, T.A., and Van Bockstaele, E.J. (2013). Coordinate regulation of noradrenergic and serotonergic brain regions by amygdalar neurons. J. Chem. Neuroanat. *52*, 9–19.

Rueckert, D., Sonoda, L.I., Hayes, C., Hill, D.L., Leach, M.O., and Hawkes, D.J. (1999). Nonrigid registration using free-form deformations: application to breast MR images. IEEE Trans. Med. Imaging *18*, 712–721.

Saper, C.B. (2006). Staying awake for dinner: hypothalamic integration of sleep, feeding, and circadian rhythms. Prog. Brain Res. *153*, 243–252.

Sena-Esteves, M., Tebbets, J.C., Steffens, S., Crombleholme, T., and Flake, A.W. (2004). Optimized large-scale production of high titer lentivirus vector pseudotypes. J. Virol. Methods *122*, 131–139.

Shammah-Lagnado, S.J., Alheid, G.F., and Heimer, L. (1996). Efferent connections of the caudal part of the globus pallidus in the rat. J. Comp. Neurol. *376*, 489–507.

Steinbusch, H.W., van der Kooy, D., Verhofstad, A.A., and Pellegrino, A. (1980). Serotonergic and non-serotonergic projections from the nucleus raphe dorsalis to the caudate-putamen complex in the rat, studied by a combined immunofluorescence and fluorescent retrograde axonal labeling technique. Neurosci. Lett. *19*, 137–142.

Stratford, T.R., and Wirtshafter, D. (1990). Ascending dopaminergic projections from the dorsal raphe nucleus in the rat. Brain Res. *511*, 173–176.

Tamura, S., Morikawa, Y., Iwanishi, H., Hisaoka, T., and Senba, E. (2004). Foxp1 gene expression in projection neurons of the mouse striatum. Neuroscience *124*, 261–267.

Trulson, M.E., and Jacobs, B.L. (1979). Raphe unit activity in freely moving cats: correlation with level of behavioral arousal. Brain Res. *163*, 135–150.

Varga, V., Székely, A.D., Csillag, A., Sharp, T., and Hajós, M. (2001). Evidence for a role of GABA interneurones in the cortical modulation of midbrain 5-hydroxytryptamine neurones. Neuroscience *106*, 783–792.

Varga, V., Kocsis, B., and Sharp, T. (2003). Electrophysiological evidence for convergence of inputs from the medial prefrontal cortex and lateral habenula on single neurons in the dorsal raphe nucleus. Eur. J. Neurosci. *17*, 280–286.

Veasey, S.C., Fornal, C.A., Metzler, C.W., and Jacobs, B.L. (1997). Single-unit responses of serotonergic dorsal raphe neurons to specific motor challenges in freely moving cats. Neuroscience *79*, 161–169.

Vertes, R.P. (1991). A PHA-L analysis of ascending projections of the dorsal raphe nucleus in the rat. J. Comp. Neurol. *313*, 643–668.

Vertes, R.P. (2004). Differential projections of the infralimbic and prelimbic cortex in the rat. Synapse *51*, 32–58.

Vertes, R.P., and Linley, S.B. (2008). Efferent and afferent connections of the dorsal and median raphe nuclei in the rat. In Serotonin and Sleep: Molecular, Functional and Clinical Aspects, J.M. Monti, S.R. Pandi-Perumal, B.L. Jacobs, and D.J. Nutt, eds. (Basel: Verlag/Switzerland), pp. 69–102.

Vertes, R.P., Linley, S.B., and Hoover, W.B. (2010). Pattern of distribution of serotonergic fibers to the thalamus of the rat. Brain Struct. Funct. *215*, 1–28.

Wall, N.R., Wickersham, I.R., Cetin, A., De La Parra, M., and Callaway, E.M. (2010). Monosynaptic circuit tracing in vivo through Cre-dependent targeting and complementation of modified rabies virus. Proc. Natl. Acad. Sci. USA *107*, 21848–21853.

Wall, N.R., De La Parra, M., Callaway, E.M., and Kreitzer, A.C. (2013). Differential innervation of direct- and indirect-pathway striatal projection neurons. Neuron *79*, 347–360.

Warden, M.R., Selimbeyoglu, A., Mirzabekov, J.J., Lo, M., Thompson, K.R., Kim, S.Y., Adhikari, A., Tye, K.M., Frank, L.M., and Deisseroth, K. (2012). A prefrontal cortex-brainstem neuronal projection that controls response to behavioural challenge. Nature *492*, 428–432.

Watabe-Uchida, M., Zhu, L., Ogawa, S.K., Vamanrao, A., and Uchida, N. (2012). Whole-brain mapping of direct inputs to midbrain dopamine neurons. Neuron *74*, 858–873.

Wickersham, I.R., Lyon, D.C., Barnard, R.J., Mori, T., Finke, S., Conzelmann, K.K., Young, J.A., and Callaway, E.M. (2007). Monosynaptic restriction of transsynaptic tracing from single, genetically targeted neurons. Neuron *53*, 639–647.

Wickersham, I.R., Sullivan, H.A., and Seung, H.S. (2010). Production of glycoprotein-deleted rabies viruses for monosynaptic tracing and high-level gene expression in neurons. Nat. Protoc. *5*, 595–606.

Zhuang, X., Masson, J., Gingrich, J.A., Rayport, S., and Hen, R. (2005). Targeted gene expression in dopamine and serotonin neurons of the mouse brain. J. Neurosci. Methods *143*, 27–32.

Zingg, B., Hintiryan, H., Gou, L., Song, M.Y., Bay, M., Bienkowski, M.S., Foster, N.N., Yamashita, S., Bowman, I., Toga, A.W., and Dong, H.W. (2014). Neural networks of the mouse neocortex. Cell *156*, 1096–1111.